



CrossMark  
click for updates

Cite this: *RSC Adv.*, 2016, 6, 43626

# Morphological and swelling behavior of cellulose nanofiber (CNF)/poly(vinyl alcohol) (PVA) hydrogels: poly(ethylene glycol) (PEG) as porogen†

Zhaoyang Xu,\* Jianyu Li, Huan Zhou, Xiangdong Jiang, Chuang Yang, Fei Wang, Yuanyuan Pan, Nana Li, Xiaoyan Li, Lina Shi and Xiaomei Shi

Novel interconnected PVA-based hydrogels with controlled porous structure prepared by freezing/thawing and porogen technique are presented in this study. Three types of poly(ethylene glycol) (PEG), with various molecular weights, have been used as porogens. Cellulose nanofiber (CNF) was incorporated into PEG-modified hydrogels as the reinforcement. The influences of PEG and CNF on the microstructure, swelling behavior and thermal properties of hydrogels were investigated. The results indicated that the porosity of hydrogels was significantly increased with PEG incorporated, and the pore size increased as the increasing of PEG molecular weight. The CNF greatly improved the hydrogel connectivity. The CNF further enhanced the swelling property on the basis of the excellent improvement effect of PEG. In addition, significantly increased thermal stability was obtained with the CNF/PEG-modified hydrogels in comparison with the pure PVA hydrogels. The low cost, nontoxic, high-performance and biocompatible hydrogels may have a promising application in biomedical fields.

Received 9th February 2016

Accepted 27th April 2016

DOI: 10.1039/c6ra03620a

www.rsc.org/advances

## 1. Introduction

Hydrogels, hydrophilic three-dimensional polymeric networks, can absorb and retain high volumes of water or other biological fluids.<sup>1</sup> This ability to swell under biological conditions makes them ideal materials for biomedical applications, such as drug delivery, protein immobilization, and other biological compounds.<sup>2,3</sup> Hydrogels also have lubricating properties, low friction coefficients and high mechanical strength, like cartilage.<sup>3</sup> Hence, hydrogels hold substantial promise for creating functional engineered tissues.<sup>4</sup>

Recently considerable interests have been focused on the design and control of novel porous hydrogels, and the improvement of the morphology, spatial organization and functional levels.<sup>5,6</sup> Porous hydrogels have been found more benefits than conventional hydrogels when they are used as biomedical and tissue engineering materials.<sup>7</sup> The porosity and fine internal pores play a significant role in enhancing the total water sorption capability and the response rate by reducing the transport resistance to fabricate functional hydrogel.<sup>8–11</sup> Thus, control of hydrogels porosity and microarchitecture plays an important role in regulating engineered tissue properties.

To improve and control porous structure, several techniques were proposed, such as the porogen technique, the phase

separation technique and the gas foaming technique.<sup>12–15</sup> In a method, studied by Caykara T *et al.*,<sup>16</sup> poly(acrylamide) (PAAm) hydrogels with a macroporous network structure were prepared by using poly(ethylene glycol) (PEG) as the porogen during the polymerization reaction. The results revealed that the PEG-modified hydrogels had more pores and higher swelling ratio compared to the conventional hydrogel. Li *et al.*<sup>11</sup> reported porous PNIPAM/PEG hydrogels synthesized by a combination of *N*-isopropyl acrylamide as monomer, polyethylene glycol (PEG) as pore-forming agent and *N,N*-methylene-bis-acrylamide as crosslinking agent. The result showed that the hydrogels without PEG had a dense surface while macropores of hydrogel formed prepared by PEG agent.

Up to now, amounts of research have shown how to fabricate porous structure of hydrogels with chemical crosslinked methods by PEG as porogen. However there has been scarce research on the role of the physical architecture. Considering the chemical crosslinked gels are used as chemical crosslinking agents. These agents are not only often toxic compounds but also can affect the integrity of the substances when entrapped (*e.g.*, proteins).<sup>17,18</sup> To circumvent this problem, an alternate method involving the fabrication of nontoxic porous hydrogels should be employed. Therefore, the objective of this study was to design nontoxic porous hydrogels with improved and adjusted pores architecture by a simple and novel method. Poly(vinyl alcohol) (PVA) was chosen as the matrix to synthesize porous hydrogels in this study, taking consideration of good biocompatibility, non-toxicity and high elasticity of PVA.<sup>19–21</sup> Also, PVA hydrogels can be obtained by physical crosslinking

College of Materials Science & Engineering, Nanjing Forestry University, Nanjing, Jiangsu 210037, China. E-mail: zhaoyangxunjfu@hotmail.com; Tel: +86 2585427628

† Electronic supplementary information (ESI) available. See DOI: 10.1039/c6ra03620a

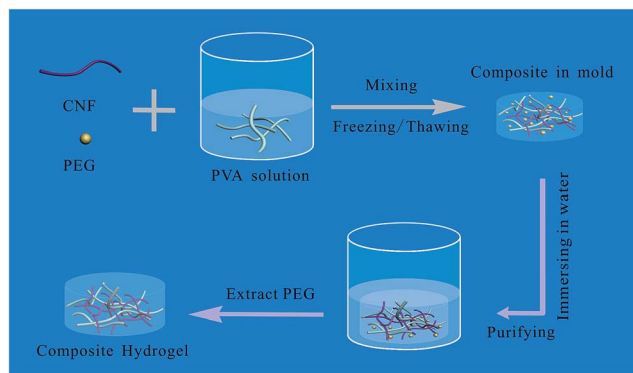


Fig. 1 Schema of PEG-modified hydrogels formation.

method and offers many advantages such as biodegradability and higher water content than other biocompatible materials.<sup>21</sup>

In the present paper, poly(vinyl alcohol) (PVA)/cellulose nanofiber (CNF) hydrogels with a controlled and highly connectivity porous structure were prepared by using poly(ethylene glycol) (PEG) with three different molecular weights as the porogen during the physically crosslinking (as shown in Fig. 1). To the best of our knowledge, there are no hydrogels based on PVA synthesized by the strategies proposed in this work. We explored the technology for controlling the porosity and microarchitecture within hydrogels. The PEG modified and CNF/PEG modified hydrogels were analyzed by swelling ratio, Fourier transform infrared spectroscopy (FTIR), scanning electron microscopy (SEM) and thermal gravimetric analysis (TGA). Those hydrogels may have potential applications in the controlled release of macromolecular active agents such as proteins and peptides, since the porous structure may be able to provide enough space for the loading and releasing of macromolecular active agents.

## 2. Materials and methods

### 2.1. Materials

Bamboo sawdust purchased from Zhejiang (Lishui, China) was sieved through a 60 mesh prior to further treatments. Poly(vinyl alcohol) with an average degree of polymerization of  $1750 \pm 50$ , 88% hydrolyzed, poly(ethylene glycol) with molecular weights of 2000, 4000 and  $6000 \text{ g mol}^{-1}$ , benzene, ethanol, sodium chlorite, glacial acetic acid, potassium hydroxide and hydrogen chloride were all obtained from Nanjing Chemical Reagent Co., Ltd. All the chemicals were used without any further treatment. De-ionized water was used throughout this research.

### 2.2. Methods

**2.2.1. Preparation of CNF.** The CNF was prepared from bamboo sawdust. It was chemically purified according to literature method of the<sup>22</sup> and adapted with appropriate modifications. First, solvent extraction was performed for the sawdust with a 2 : 1 volume ratio of benzene/ethanol mixture at  $90^\circ\text{C}$  for 6 h. Then, the sawdust was treated in an acidified sodium chlorite solution at  $75^\circ\text{C}$  for an hour, and the process was

repeated five times to remove lignin. After that, the obtained materials were added into 2.0 wt% potassium hydroxide with stirring at  $90^\circ\text{C}$  for 2 h to remove hemicelluloses, residual starch, and pectin. Then the samples were further treated with an acidified sodium chlorite solution for 1 h, and treated with 5 wt% potassium hydroxide for 2 h to obtain highly purified cellulose. Last, 1.5 wt% hydrochloric acid solution was used at  $80^\circ\text{C}$  for 2 h to degrade cellulose. Throughout the process, the samples were washed to neutral and kept in a water swollen state. After chemical treatment, CNF slurry was prepared by beating 1.0 wt% purified cellulose with a grinder (MKCA6-2, Masuko Sangyo Co., Ltd., Japan) at 1500 rpm<sup>23</sup> and stored for further utilization.

**2.2.2. Preparation of PEG modified hydrogels.** The PEG modified hydrogels were prepared by dissolving PVA (7.5 wt%) in deionized water with stirring at  $95^\circ\text{C}$  for 3 h. PEG2000 in different contents of PVA solution (0, 1, 2, 3 and 4%, w/w) and PEG4000, PEG6000 in percentage of 3%, w/w were added to this solution which will be coded as 0gPEG2 (pure PVA hydrogels), 1gPEG2, 2gPEG2, 3gPEG2, 4gPEG2, 3gPEG4 and 3gPEG6. The preparations and samples are shown in Table 1. The final mixture was maintained at  $95^\circ\text{C}$  for 1 h for complete dissolution. The resulting mixture was poured into mold and cooled down at room temperature, and then kept at  $-20^\circ\text{C}$  for 20 h. The homogeneous solution after freezing was held at room temperature ( $25^\circ\text{C}$  for 4 h). Freezing and thawing cycles were repeated 5 times to provide mechanically acceptable gels for further experiments. Here, PEG with three different molecular weights is employed as the pore-forming agent, which does not react with other chemicals during polymerization. The resulting hydrogels were purified by immersing in deionized water to extract the pore forming agent and the unreacted materials.

**2.2.3. Preparation of CNF/PEG modified hydrogels.** The CNF/PEG modified hydrogels were prepared by dissolving PVA (7.5 wt%) in CNF suspension (the CNF content was 10.0 wt% of the PVA) with stirring at  $95^\circ\text{C}$  for 3 h. PEG2000, PEG4000 and PEG6000 in percentages of 3%, w/w were added to this mixture, which were coded as CNF/PEG2, CNF/PEG4 and CNF/PEG6 (as shown in Table 1). The CNF/PEG modified hydrogels were obtained followed the same method as discussed in 2.2.2.

## 3. Characterizations

### 3.1. Scanning electron microscopy

The morphology of freeze-dried CNF and hydrogels was investigated by SEM. Hydrogels were swollen completely in deionized water at  $25^\circ\text{C}$  and freeze-dried at  $-43^\circ\text{C}$  under a vacuum of 1 Pa for 48 h to avoid the collapse of porous structure. The freeze-dried samples were frozen in liquid nitrogen and snapped immediately, and coated with gold for 60 s. Finally, the fracture surfaces of the hydrogels were determined by a Hitachi S-4800 using 5.0 kV secondary electrons.

### 3.2. Pore analysis

Pore analysis was performed using the public domain ImageJ software developed at the US National Institutes of Health (NIH)

Table 1 Preparation conditions for PEG-modified hydrogels

Sample code	PVA (wt%)	PEG2000 (wt%)	PEG4000 (wt%)	PEG6000 (wt%)	Weight ratio CNF : PVA
Pure PVA	7.5	0	0	0	0
1gPEG2	7.5	1	0	0	0
2gPEG2	7.5	2	0	0	0
3gPEG2	7.5	3	0	0	0
4gPEG2	7.5	4	0	0	0
3gPEG4	7.5	0	3	0	0
3gPEG6	7.5	0	0	3	0
CNF/PEG2	7.5	3	0	0	10
CNF/PEG4	7.5	0	3	0	10
CNF/PEG6	7.5	0	0	3	10

(available at <http://rsb.info.nih.gov/ij/>).<sup>24</sup> ImageJ software, developed by Wayne Rasband at NIH, was used to measure the sample pores selected on SEM images for each type of sample. The sum areas of the pores were divided by the total exposed area of the sample to obtain porosity percentage. Results are presented as means  $\pm$  SEM of three experiments.

### 3.3. Fourier transforms infrared spectroscopy

FTIR spectra (4000–500  $\text{cm}^{-1}$ ) of the CNF and hydrogels were acquired using a Nicolet iS10 (Thermo Electron Corp. USA) at 4  $\text{cm}^{-1}$  resolution and 32 scans at room temperature. All the hydrogels samples were freeze-dried and have equal thickness before analyzed.

### 3.4. Swelling measurements

Swelling properties of hydrogels were evaluated through dynamic swelling studies which were measured by the classical gravimetric method. The hydrogels were dried in a vacuum oven 50  $^{\circ}\text{C}$  for 24 h to determine their dry weight ( $W_d$ ). Then, the dried samples were immersed in distilled water at 25  $^{\circ}\text{C}$ , and removed from water at regular time intervals. The excess water on their surface was wiped quickly by filter papers and weighing ( $W_t$ ). This procedure was repeated three times to gain the average value. The swelling ratio (SR) was defined as:

$$\text{SR} = [(W_t - W_d)/W_d] \times 100\% \quad (1)$$

where  $W_t$  is weight of the swollen sample at time  $t$ ,  $W_d$  is the weight of sample at dry state.

### 3.5. Thermal gravimetric analysis

Thermal properties of the hydrogels were characterized by thermogravimetric analysis (TGA, 209F3, NETSCH, Germany). The dry samples weighing between 3 and 10 mg were packed in aluminum pans and tested in the range of 30–600  $^{\circ}\text{C}$  at a heating rate of 10  $^{\circ}\text{C min}^{-1}$  under nitrogen atmosphere.

## 4. Results and discussion

### 4.1. FTIR

The formation mechanism of PVA hydrogel is generally considered that, the crystallization of the aqueous PVA phase

occur during freezing/thawing cycles at low temperature and the subsequent alignment of the polymer chains in the liquid part of the PVA, which then hydrogen bond to each other.<sup>3,25</sup> Intrachain physical cross-links are formed between the PVA hydroxyl groups and interchain cross-links form between the hydroxyl groups of PVA and CNF. The FTIR spectra of the traditional and PEG-modified hydrogels are shown in Fig. 2. The exists of a typical absorption peak (1143  $\text{cm}^{-1}$ ), which belongs to the C–C stretching vibration of PVA and associated with the crystallinity of PVA, including C–O at 1088  $\text{cm}^{-1}$  vibration in each spectrum of hydrogels.<sup>26,27</sup> The spectra of the PVA and PEG-modified hydrogels are almost similar. In this aspect, if there exists PEG in the modified hydrogels, a typical and strong absorption peak positioned at 1096  $\text{cm}^{-1}$  (Fig. 2a), which belongs to the C–O stretch of PEG, would appear in the difference spectra of PEG-modified hydrogels. However, it is clear that no obvious peak appearing at 1096  $\text{cm}^{-1}$  in the spectra of the PEG-modified hydrogels,<sup>11,28</sup> indicating that the

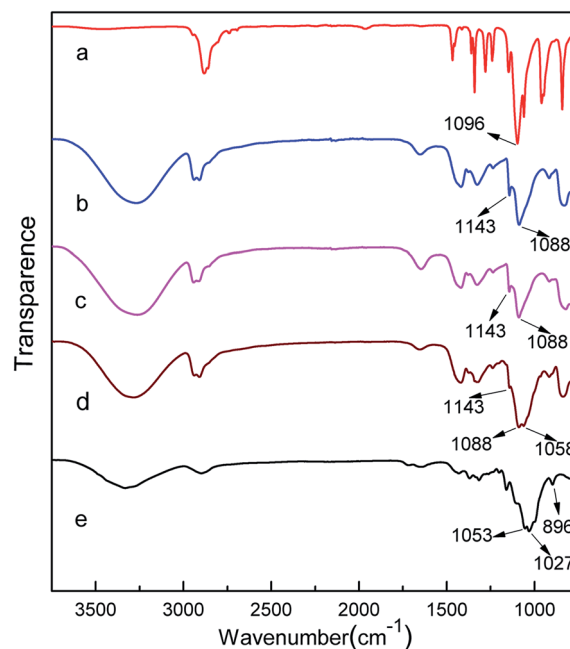


Fig. 2 FTIR spectra of the samples: (a) PEG, (b) pure PVA hydrogels, (c) PEG-modified hydrogels, (d) CNF/PEG-modified hydrogels, (e) CNF.

modified hydrogels have the same chemical composition as the traditional PVA hydrogel and PEG do not exist in the modified hydrogels after it is extensively washed. PEG acts as the pore-forming agent do not participate in the polymerization. The absorption peaks in the spectra of CNF at 1053, 1027 and 896  $\text{cm}^{-1}$ , arose from C–O, O–C–O stretching vibrations and anomeric carbon of  $\beta$ -D-glucopyranosyl of cellulose, respectively.<sup>27</sup> During the process of the freezing/thawing, intra-chain physical cross-links are formed between the hydroxyl groups of PVA, and inter-chain cross-links form between the hydroxyl groups of PVA and CNF. On the other hand, the peak position of the C–O stretching vibration of cellulose shifted, which might contribute to the expected interaction of the hydrophilic surfaces of CNF with hydroxyl groups of PVA.<sup>29,30</sup>

#### 4.2. Morphology

Fig. 3 shows the SEM image of freeze-dried CNF sample, which formed a porous network structure with pore size range from 20 to 170 nm. And diameter range of CNF was from 10 to 30 nm. The SEM images were taken at random locations across cross-sections of the hydrogels, and the values of pore size and porosity generated from three images were used to calculate the average pore size and porosity for each sample. Thus, the standard deviation of the porosity and pore size (Table 2) are an indication of homogeneity of pore distribution. The SEM images of cross-sections of PVA hydrogels in different formulations are shown in Fig. 4. A rough surface morphology with a few irregular pores was seen in the image of the pure PVA

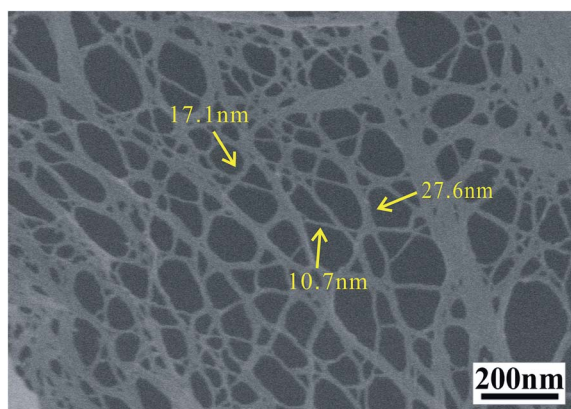


Fig. 3 SEM images of CNF.

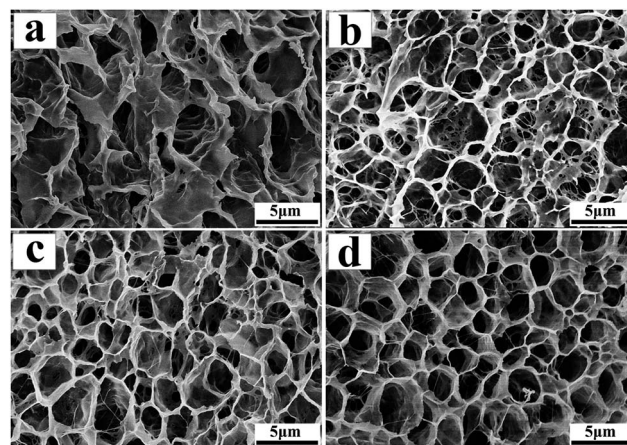


Fig. 4 SEM images of hydrogel samples: (a) pure PVA, (b) 1gPEG2, (c) 2gPEG2, and (d) 4gPEG2.

hydrogels (Fig. 4a), but no discernible pores network were detected in the images. By adding PEG, PEG-modified hydrogels exhibit a porous microstructure (Fig. 4b–d). There was obvious difference of the uniformity of the pores for different content of PEG in PVA hydrogels. With increase of the PEG content from 1 to 4 wt%, more and more uniform pores appeared. This could be explained that during the freezing stage, porous structure is generated after the phase separation of the homogeneous polymer solution. The hydration and the exclusion volume of PEG may provide spatial hindrance during the crosslinking process.<sup>28,31</sup> Thus, a more porous structure with uniform pores is formed with the PEG-modified hydrogels.

The SEM images of cross-sections of hydrogels with varying molecular weight of PEG and PEG-modified hydrogels with CNF are presented in Fig. 5. It can be seen from Fig. 5 that all samples have a well-defined pore network. But there was obvious difference of the number and size of pores with varying molecular weight of PEG in PVA hydrogels. Generally, the pores had a circular structure but varied greatly in diameter with different hydrogels type (this will be discussed in the next paragraph). There are two possible reasons. First, due to the presence of PEG, phase separation of formed PVA chains occurs during the polymerization, leading to micro-porous structures.<sup>28</sup> Second, the average diameter of PEG molecules in aqueous media increases with an increase in PEG molecular weight; the higher the molecular weight of

Table 2 Pore size and porosity of hydrogels, determined using imageJ analysis of SEM images

	PEG2000				PEG2000		PEG4000		PEG6000	
	Pure PVA	1g	2g	4g	3g	/CNF	3g	/CNF	3g	/CNF
Distribution range ( $\mu\text{m}$ )	1.14–3.07	1.27–2.37	1.19–2.24	1.49–2.82	1.37–2.05	1.25–2.16	1.75–2.97	1.64–3.05	2.06–3.82	2.26–3.65
Average pore size ( $\mu\text{m}$ )	1.97 $\pm$ 0.61	1.82 $\pm$ 0.43	1.76 $\pm$ 0.32	1.80 $\pm$ 0.47	1.69 $\pm$ 0.34	1.78 $\pm$ 0.30	2.33 $\pm$ 0.38	2.35 $\pm$ 0.41	3.05 $\pm$ 0.53	3.01 $\pm$ 0.42
Pore area (%)	31.2 $\pm$ 5.8	50.4 $\pm$ 4.7	54.6 $\pm$ 3.7	63.6 $\pm$ 3.9	56.9 $\pm$ 4.4	55.8 $\pm$ 4.5	60.8 $\pm$ 3.5	62.5 $\pm$ 2.2	62.6 $\pm$ 2.6	62.5 $\pm$ 4.1

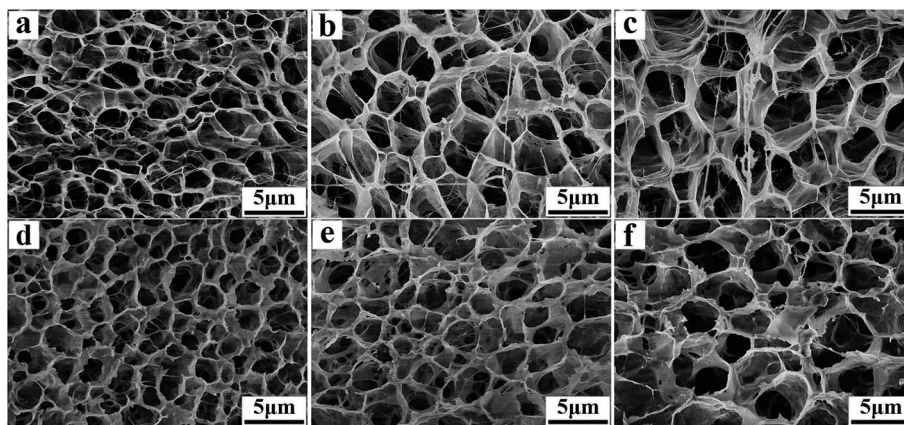


Fig. 5 SEM images of hydrogel samples: (a) PEG2, (b) PEG4, (c) PEG6, (d) CNF/PEG2, (e) CNF/PEG4, and (f) CNF/PEG6.

PEG applied during the polymerization, the larger pores formed in the resultant hydrogels.<sup>16</sup> Moreover, the PVA hydrogels with CNF presented a more interconnected pores structure (such as Fig. 5b and e), which is more beneficial to mass transfer.

Porosity and pore size were evaluated using ImageJ, and the values obtained for each sample type are listed in Table 2. From the values of porosity, it was concluded that porosity increased significantly with the addition of PEG compared to the pure PVA hydrogels ( $p = 31.2 \pm 5.8$ ). And the porosity increased (from  $50.4 \pm 4.7$  to  $63.6 \pm 3.9$ ) with the increasing content of PEG, but the pore size distribution and average pore size were not much affected by PEG content (Table 2). These agree well with the SEM results that PEG content only affect the pores uniformity. With increasing molecular weight of PEG the pores size of PVA hydrogels became increasingly large (Table 2). The porosity was not much affected by molecular weight of PEG except for the PEG2000, compared the three type hydrogels (varying molecular weight of PEG-modified). This might be attributed to the fact that irregular pores of PVA/PEG2 hydrogels affect the porosity.

It was noteworthy that there were no statistically significant differences of the porosity and pore size with the incorporation of CNF into hydrogels. As the results of the swelling experiments discussed below, it can be seen that the swelling ratio of all the CNF/PEG-modified hydrogels were higher than the corresponding PEG-modified hydrogels in each of the same time periods, which suggested that the water absorption rate of the CNF/PEG-modified hydrogels were also higher. Also, the pore size, pore morphology and interconnectivity are interrelated and influence the permeability of fluid through hydrogels. So the increment of the water absorption rate of the CNF/PEG-modified hydrogels was mainly related to the increased degree of connectivity of the pore structure. Besides, the SEM images were taken at random locations across cross-sections of the hydrogels. So in a homogeneous hydrogel, the pore structure at random locations inside of hydrogel is similar. The CNF/PEG-modified hydrogels mainly present an interpenetrating porous structure. Thus, in view of the above results and combining with the observation of SEM images, a conclusion can be drawn that

the CNF only has a great influence on the connectivity of the pore structure.

#### 4.3. Swelling

The swelling behaviors of PVA and PEG-modified hydrogels were shown in Table 3 and Fig. 6. It can be seen that all the samples absorbed water rapidly in the initial swelling stage, and the swelling ratio increased dramatically with time. The water absorption of all PEG-modified hydrogels was more quickly than the conventional PVA hydrogels, it could be explained that more porous structures make water molecules transfer easier between the hydrogels matrix and the external aqueous phase. Also, the resultant rough skin layer of pure PVA hydrogels acts as a barrier for further water permeation and prevents the freed water diffusion out from the gels matrix.<sup>32</sup>

The water absorption rate and equilibrium swelling ratio of hydrogels were increased with the increased content of PEG. The equilibrium swelling rate of PVA hydrogels was improved from 580% in absence of PEG to 930% in presence of 4 wt% PEG2000 (Table 3), indicating that more content of PEG could improve the water absorption capacity of PVA hydrogels because of improved porosity. Fig. 6b displayed the swelling behaviors of the PEG-modified and CNF/PEG-modified samples with varying molecular weight of PEG after dried in vacuum oven at 60 °C for 24 h. In order to observe more clearly, Fig. 6b is divided into three parts (see ESI data, Fig. S1†). It can be seen that the water absorption rate and equilibrium swelling rate increased with increasing molecular weight of PEG, indicating that higher molecular weight of PEG could produce larger pores in the hydrogels. Fig. 6b also implies that the CNF/PEG-modified hydrogels have better swellability. All the CNF/PEG-modified hydrogels exhibited a larger swelling ratio than PEG-modified according to the molecular weight of PEG. For example, the PEG6000-modified hydrogels had about 800% swelling ratio within 30 min, or 910% within 300 min, whereas the CNF/PEG6000-modified hydrogels had about 900% and 1040%, respectively, within the same time frames. This was attributed to the hydrophilic nature of CNF and interpenetrating network structure caused by CNF in the PVA hydrogels, leading to the increase of swelling degree.

Table 3 The equilibrium swelling ratio of hydrogels

	PEG2000			PEG2000		PEG4000		PEG6000		
	Pure PVA	1g	2g	4g	3g	/CNF	3g	/CNF	3g	/CNF
Equilibrium SR (%)	588 ± 9.0	715 ± 5.3	792 ± 7.3	935 ± 11.1	858 ± 11.3	927 ± 10.1	950 ± 8.7	1040 ± 2.6	1008 ± 12.2	1125 ± 9.6

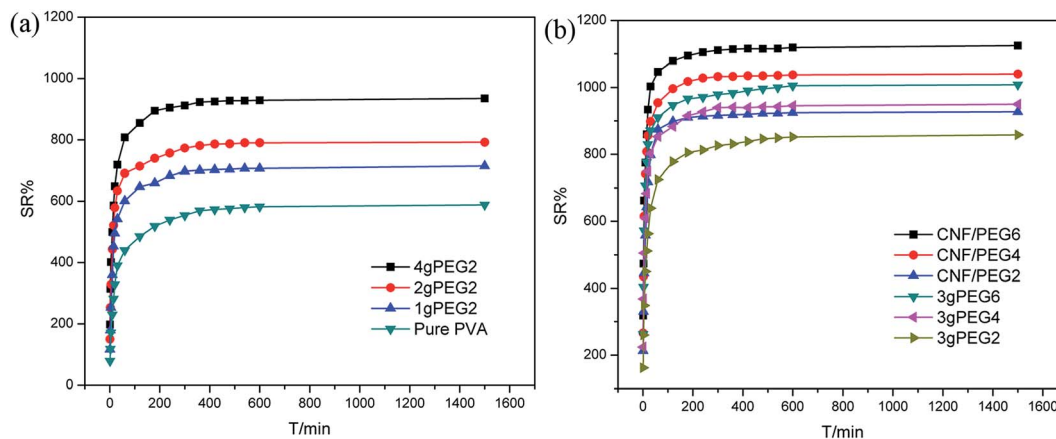


Fig. 6 Swelling properties of hydrogels with different formulations: (a) PEG-modified hydrogels, (b) CNF/PEG-modified hydrogels.

The swellability of hydrogels cannot be simply related to the degree of porosity, since the micro-architecture of the porous network may also play an important role in controlling the capacity of water sorption, as suggested by Sannino *et al.*<sup>33</sup> In another work, Zhuo *et al.*<sup>34</sup> reported that there are two dominant factors that determine the responsive kinetics of porous hydrogels. One is the gels surface area in contact with water molecules, and the other is the average diameter of water channels (pore size) formed by the porous structure in gels matrix. Increasing the average diameter of the water channels makes it easier for water molecules to enter the hydrogels network. For porous hydrogels the pore geometry also influenced water uptake.<sup>35</sup> Indeed, the pore size, pore morphology and interconnectivity are interrelated and influence the permeability of fluid through hydrogels.<sup>36</sup> Enlargement of the pore size during gel swelling, and therefore the amount of bulky water, depends not only on the initial size of the pore but also on its shape and the degree of interconnectivity.<sup>25</sup> Therefore, an increased PEG molecular weight and PEG content yields a hydrogel with a larger pore size and a more uniform porous structure, resulting in larger equilibrated swelling ratios. Also, the connectivity of porous structure improved with CNF incorporated into PVA/PEG hydrogels, thus having a great positive effect on swelling. Fig. 7 is the transmission path models of water molecule in porous structure of hydrogels. Combined with the results of the swelling and morphology behavior, the connectivity of porous structure of the CNF/PEG-modified hydrogels was increased compared with the PEG-modified hydrogels. The main purpose of schematic was mainly to express the effect of interpenetrating porous structure. As the model shown, the water molecules have different transmission path to go through the porous structure when hydrogels are

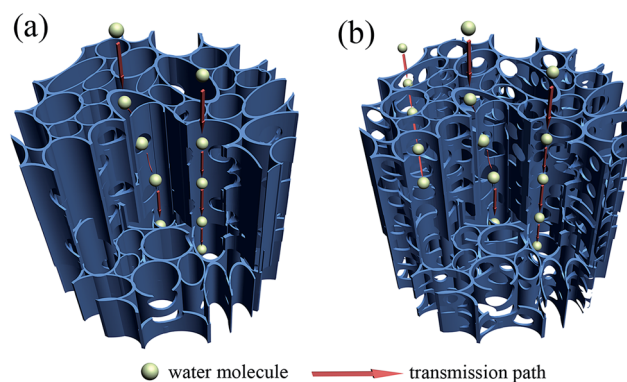


Fig. 7 The transmission path models of water molecule in porous structure of hydrogels: (a) PEG-modified hydrogels, (b) CNF/PEG-modified hydrogels.

swelling in the water. Due to the porous structure of PEG-modified (Fig. 7a), some water molecules can go straight into the hydrogels, but the distribution and direction of pores still limit the transmission of water molecules. However, the structure with high connectivity of CNF/PEG-modified (Fig. 7b) provides much more space and diffusion channels for water molecules. These spaces and channels greatly reduces the transport resistance of water molecules, shorten the time for water molecules motion, and greatly improves the swelling properties and mass transfer of hydrogels.

#### 4.4. Thermal analysis

In view of the importance of thermal stability of composite materials in many applications, thermal decomposition of the

different hydrogels was examined. The TGA thermographs of PVA based hydrogels as a function of various PEG and CNF contents are shown in Fig. S2 (see ESI data, Fig. S2†). The relative thermal stabilities of the different hydrogels were evaluated by comparing the weight loss within a temperature 30–600 °C. From Fig. S2a,† it can be observed that all samples exhibited three distinct weight loss stages. The first weight loss stage at 30–235 °C (5 wt% loss) can be ascribed to the removal of residual water in the network. The second phase at 235–380 °C is accompanied with a decomposition of side chain of PVA. And the third stage at 380–500 °C is due to the decomposition of main chain of PVA.<sup>27</sup> There was no significant difference in thermal decomposition between pure PVA and PEG-modified hydrogels, indicating PEG as porogen has no effect on the thermal stability of PVA hydrogels.

As shown in Fig. S2b,† major weight losses of about 80 wt% were observed in the range of 300–500 °C for all CNF/PEG-modified samples, which corresponds to the structural decomposition of PVA and thermal degradation of CNF. Over about 500 °C, the TGA curves of all samples became flat, mainly the inorganic residue remained.<sup>19,27</sup> As mentioned above, the onset decomposition temperature of PVA hydrogels is about 235 °C, while the onset decomposition temperatures of CNF/PEG-modified hydrogels shift to 300 °C (Fig. S2b†). The addition of CNF to PVA hydrogels showed a significant effect on the thermal deformation, thus confirming the enhanced thermal stability due to a strong hydrogen bonding between the hydroxyl groups of CNF and the PVA.<sup>27</sup>

## 5. Conclusion

In conclusion, novel PEG-modified CNF/PVA hydrogels with controlled porous structure was successfully prepared with varying molecular weight of PEG. The morphological data from SEM revealed that introduction of PEG as porogen in the physically crosslinked PVA hydrogels significantly affected the structure of the hydrogels. The porous structure appeared and pores became more uniform with increased content of PEG. Also pores size of PEG-modified hydrogels increased with molecular weight of PEG increased. Furthermore, the swelling properties were greatly improved due to the presence of porous structure. After adding CNF into PEG-modified hydrogels, a highly porous and interconnected matrix with enhanced swelling and thermal properties was formed. They are promising hydrogels for application in the controlled release and other functional engineering fields.

## Acknowledgements

This work was supported by the National Natural Science Foundation of China (Grant No. 31300483), the Natural Science Foundation of Jiangsu Province of China (Grant No. BK20130971) and a Project Funded by the Priority Academic Program Development of Jiangsu Higher Education Institutions (PAPD). We acknowledge Advanced Analysis & Testing Center of Nanjing Forestry University.

## References

- 1 M. Karg and T. Hellweg, New “smart” poly(NIPAM) microgels and nanoparticle microgel hybrids: properties and advances in characterization, *Curr. Opin. Colloid Interface Sci.*, 2009, **14**(6), 438–450.
- 2 C. Mallikarjuna, V. H. Bhaskar, J. M. Kumar, *et al.* Review on Hydrogel-A Novel Carrier, *PharmaTutor Mag.*, 2014, **2**(6), 42–51.
- 3 K. L. Spiller, S. J. Laurencin, D. Charlton, *et al.* Superporous hydrogels for cartilage repair: evaluation of the morphological and mechanical properties, *Acta Biomater.*, 2008, **4**(1), 17–25.
- 4 N. Annabi, J. W. Nichol, X. Zhong, *et al.* Controlling the porosity and microarchitecture of hydrogels for tissue engineering, *Tissue Eng.*, 2010, **16**(4), 371–383.
- 5 Q. Zhao, J. Sun, X. Wu, *et al.* Macroporous double-network cryogels: formation mechanism, enhanced mechanical strength and temperature/pH dual sensitivity, *Soft Matter*, 2011, **7**(9), 4284–4293.
- 6 E. S. Dragan, M. M. Perju and M. V. Dinu, Preparation and characterization of IPN composite hydrogels based on polyacrylamide and chitosan and their interaction with ionic dyes, *Carbohydr. Polym.*, 2012, **88**(1), 270–281.
- 7 M. V. Dinu, M. Přádný, E. S. Drăgan, *et al.* Ice-templated hydrogels based on chitosan with tailored porous morphology, *Carbohydr. Polym.*, 2013, **94**(1), 170–178.
- 8 B. B. Mandal and S. C. Kundu, Cell proliferation and migration in silk fibroin 3D scaffolds, *Biomaterials*, 2009, **30**(15), 2956–2965.
- 9 S. M. Lien, L. Y. Ko and T. J. Huang, Effect of pore size on ECM secretion and cell growth in gelatin scaffold for articular cartilage tissue engineering, *Acta Biomater.*, 2009, **5**(2), 670–679.
- 10 Y. Zhang and L. Ye, Improvement of permeability of poly(vinyl alcohol) hydrogel by using poly(ethylene glycol) as porogen, *Polym.-Plast. Technol. Eng.*, 2011, **50**(8), 776–782.
- 11 Z. Li, W. Liu, Z. Li, *et al.* Swelling and thermal properties of porous PNIPAM/PEG hydrogels prepared by radiation polymerization, *Nucl. Sci. Tech.*, 2013, **2**, 005.
- 12 J. Chen, H. Park and K. Park, Synthesis of superporous hydrogels: hydrogels with fast swelling and superabsorbent properties, *J. Biomed. Mater. Res.*, 1999, **44**(1), 53–62.
- 13 H. G. Kang, S. B. Lee and Y. M. Lee, Novel preparative method for porous hydrogels using overrun process, *Polym. Int.*, 2005, **54**(3), 537–543.
- 14 Q. Liu, E. L. Hedberg, Z. Liu, *et al.* Preparation of macroporous poly(2-hydroxyethyl methacrylate) hydrogels by enhanced phase separation, *Biomaterials*, 2000, **21**(21), 2163–2169.
- 15 T. S. Karande, J. L. Ong and C. M. Agrawal, Diffusion in musculoskeletal tissue engineering scaffolds: design issues related to porosity, permeability, architecture, and nutrient mixing, *Ann. Biomed. Eng.*, 2004, **32**(12), 1728–1743.
- 16 T. Caykara, M. Bulut, N. Dilsiz, *et al.* Macroporous poly(acrylamide) hydrogels: swelling and shrinking

- behaviors, *J. Macromol. Sci., Pure Appl. Chem.*, 2006, **43**(6), 889–897.
- 17 E. Fathi, N. Atyabi, M. Imani, *et al.* Physically crosslinked polyvinyl alcohol–dextran blend xerogels: morphology and thermal behavior, *Carbohydr. Polym.*, 2011, **84**(1), 145–152.
- 18 J. Berger, M. Reist, J. M. Mayer, *et al.* Structure and interactions in chitosan hydrogels formed by complexation or aggregation for biomedical applications, *Eur. J. Pharm. Biopharm.*, 2004, **57**(1), 35–52.
- 19 E. R. Kenawy, E. A. Kamoun, M. S. M. Eldin, *et al.* Physically crosslinked poly(vinyl alcohol)-hydroxyethyl starch blend hydrogel membranes: synthesis and characterization for biomedical applications, *Arabian J. Chem.*, 2014, **7**(3), 372–380.
- 20 S. Jiang, Z. Su, X. Wang, *et al.* Development of a new tissue-equivalent material applied to optimizing surgical accuracy, *Mater. Sci. Eng., C*, 2013, **33**(7), 3768–3774.
- 21 E. A. Kamoun, X. Chen, M. S. M. Eldin, *et al.* Crosslinked poly(vinyl alcohol) hydrogels for wound dressing applications: a review of remarkably blended polymers, *Arabian J. Chem.*, 2015, **8**(1), 1–14.
- 22 W. Chen, H. Yu and Y. Liu, Preparation of millimeter-long cellulose I nanofibers with diameters of 30–80nm from bamboo fibers, *Carbohydr. Polym.*, 2011, **86**(2), 453–461.
- 23 K. Abe and H. Yano, Comparison of the characteristics of cellulose microfibril aggregates isolated from fiber and parenchyma cells of Moso bamboo (*Phyllostachys pubescens*), *Cellulose*, 2010, **17**(2), 271–277.
- 24 W. Rasband, ImageJ. Bethesda (MD): National Institutes of Health, 1997.
- 25 A. Autissier, V. C. Le, C. Pouzet, *et al.* Fabrication of porous polysaccharide-based scaffolds using a combined freeze-drying/cross-linking process, *Acta Biomater.*, 2010, **6**(9), 3640–3648.
- 26 H. Tadokoro, S. Seki and I. Nitta, Some information on the infrared absorption spectrum of polyvinyl alcohol from deuteration and pleochroism, *J. Polym. Sci.*, 1956, **22**(102), 563–566.
- 27 D. Liu, X. Sun, H. Tian, *et al.* Effects of cellulose nanofibrils on the structure and properties on PVA nanocomposites, *Cellulose*, 2013, **20**(6), 2981–2989.
- 28 G. B. Demirel, T. Caykara, M. Demiray, *et al.* Effect of pore-forming agent type on swelling properties of macroporous poly(*N*-[3-(dimethylaminopropyl)]-methacrylamide-co-acrylamide) hydrogels, *J. Macromol. Sci., Phys.*, 2008, **46**(1), 58–64.
- 29 T. Abitbol, T. Johnstone, T. M. Quinn, *et al.* Reinforcement with cellulose nanocrystals of poly(vinyl alcohol) hydrogels prepared by cyclic freezing and thawing, *Soft Matter*, 2011, **7**(6), 2373–2379.
- 30 E. F. Reis, F. S. Campos, A. P. Lage, *et al.* Synthesis and characterization of poly(vinyl alcohol) hydrogels and hybrids for rMPB70 protein adsorption, *J. Mater. Res.*, 2006, **9**(2), 185–191.
- 31 Y. C. Chiu, S. Kocagoz, J. C. Larson, *et al.* Evaluation of physical and mechanical properties of porous poly(ethylene glycol)-co-(l-lactic acid) hydrogels during degradation, *PLoS One*, 2013, **8**(4), e60728.
- 32 T. Caykara, M. Bulut, N. Dilsiz, *et al.* Macroporous poly(acrylamide) hydrogels: swelling and shrinking behaviors, *J. Macromol. Sci., Pure Appl. Chem.*, 2006, **43**(6), 889–897.
- 33 A. Sannino, P. A. Netti, G. Mensitieri, *et al.* Designing microporous macromolecular hydrogels for biomedical applications: a comparison between two techniques, *Compos. Sci. Technol.*, 2003, **63**(16), 2411–2416.
- 34 R. X. Zhuo and W. Li, Preparation and characterization of macroporous poly(*N*-isopropylacrylamide) hydrogels for the controlled release of proteins, *J. Polym. Sci., Part A: Polym. Chem.*, 2003, **41**(1), 152–159.
- 35 S. Van Vlierberghe, V. Cnudde, B. Masschaele, *et al.* Porous gelatin cryogels as cell delivery tool in tissue engineering, *J. Controlled Release*, 2006, **116**(2), e95–e98.
- 36 E. A. Sander and E. A. Nauman, Permeability of musculoskeletal tissues and scaffolding materials: experimental results and theoretical predictions, *Crit. Rev. Bioeng.*, 2003, **31**(1–2), 1–26.
- 37 S. Y. Lee, D. J. Mohan, I. A. Kang, *et al.* Nanocellulose reinforced PVA composite films: effects of acid treatment and filler loading, *Fibers Polym.*, 2009, **10**(1), 77–82.